Ni-Base Superalloys: Alloying and Microstructural Control

Shi Qiu and Zengbao Jiao*

Department of Mechanical Engineering, The Hong Kong Polytechnic University, Hong Kong, China

*Corresponding author: zb.jiao@polyu.edu.hk

1. Introduction

Ni-based superalloys have been widely used for high-temperature applications in aerospace, automotive, and power plants due to their superior creep resistance and excellent high-temperature strength [1-3]. Since the development of the first Ni-based superalloys in the 1940s, these materials have been in continuous development to optimize the creep, fatigue, and corrosion resistance for service at temperatures of above 1100 °C [4-7].

Ni-based superalloys consist of ordered $L1_2$ γ′ precipitates and disordered face-centered cubic (FCC) γ matrix. The γ′ precipitates are embedded in the γ matrix, and the two phases share coherent interfaces. This unique dual-phase microstructure contributes to excellent mechanical properties of Ni-based superalloys during long-term thermal exposure, which is related to the inhibition of dislocation motion originating from dense dislocation networks at the γ/γ′ interface. The control of microstructure parameters in Ni-based superalloys can be achieved by the grain boundary engineering and the changing of volume fraction, size, and shape of γ′ phase.

In addition to Ni and Al, Ni-based superalloys also contains a series of other alloying elements, such as Ta, Ti, Co, Cr, Mo, Re, W, and Ru. Cr, Co, Mo, W, Re, and Ru prefer to partitioning into the γ matrix, which can be referred to as γ-stabilizing elements, whereas Ta and Ti tend to partition to the γ′ phase. With rational composition design, the improvement of high-temperature performance can achieve by tailoring the precipitate microstructure and intrinsic parameters of the γ and γ′ phases, such lattice misfit, anti-phase boundary (APB) energy, stacking fault energy, elastic modulus, and solidus and liquidus temperatures. Therefore, understanding the relationship between chemical composition, microstructure, and high-temperature performance is essential for the design of new-generation superalloys with higher-temperature capabilities. This chapter systematically reviews the microstructures, alloying effects, thermal stability, and creep resistance of Ni-based superalloys.

2. Microstructure

2.1. Precipitate microstructure

Ni and Al are the two basic elements in Ni-based superalloys. In the binary Ni-Al phase diagram, Ni_3Al can form as a second precipitate phase. Figure 1a shows the crystal structure of the γ′ and γ phases. The γ′-Ni_3Al phase has a $L1_2$ structure, which can be coherent with the γ phase. During the coarsening process, the γ′ precipitate form a cuboidal morphology to minimize the strain energy by aligning the interfaces parallel to the elastically soft <100> directions [8]. The typical γ/γ′ microstructure of Ni-based superalloys is displayed in Fig. 1b [9]. The two phases share coherent interfaces, and the γ matrix is in narrow parallel channels between the γ′ cuboids. The volume fraction of γ′ phase is usually in the range of 60-80% [10]. Considering the solubility of Al in Ni is 15 at.% at 1100 °C [11], other γ′-forming elements, such as Ti and Ta, are often added to promote the formation of γ′ phase. To improve the high-temperature performance, refractory elements, such as W, Mo, Re, and Ru, are often added to Ni-based superalloys. Figure 1c shows the elemental distribution in a Ni-based superalloy [9]. Cr, Re, Co, and Mo prefer to partition into the γ matrix, whereas Al, Ta, and Ti tend to partition to the γ′ precipitates.

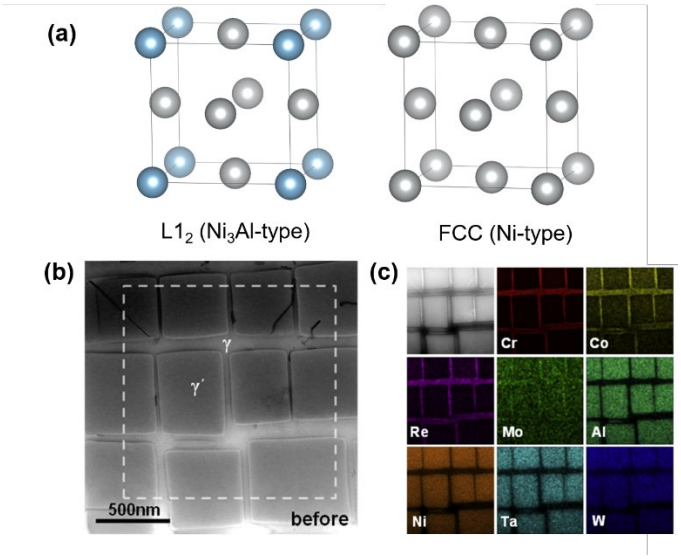

Fig. 1. Microstructures of Ni-based superalloys. (a) Schematic diagram of the $L1_2$ and FCC structures., (b) morphology of the γ/γ′ microstructure, and (c) elemental distributions. [9]

As compared with the γ or γ′ single phase, the γ/γ′ dual-phase structure exhibits a better creep performance. The minimum creep rate of the γ, γ′ and γ/γ′ dual-phase structures in a series of Ni-based superalloys is shown in Fig. 2, and the chemical compositions of the alloys are listed in Table 1 [12-18]. Under the same applied stress, the minimum creep rate of the γ/γ′ dual-phase structure is much lower than that of the single-phase structures, illustrating the superior creep resistance of the γ/γ′ dual-phase microstructure. The low minimum creep rate of the dual-phase microstructure is related to the interfacial dislocations at the γ/γ′ interface [19]. The dislocations propagate at the γ/γ′ interface, leading to the dense dislocation networks. In the secondary creep stage, the interfacial dislocation networks become stable, which effectively impede the dislocation motion. As a result, the minimum creep rate decreases. Studies show that adding Ru and Mo results in a large misfit between the γ and γ′ phases, which leads to the formation of dense dislocation networks at the γ/γ′ interface[20, 21].

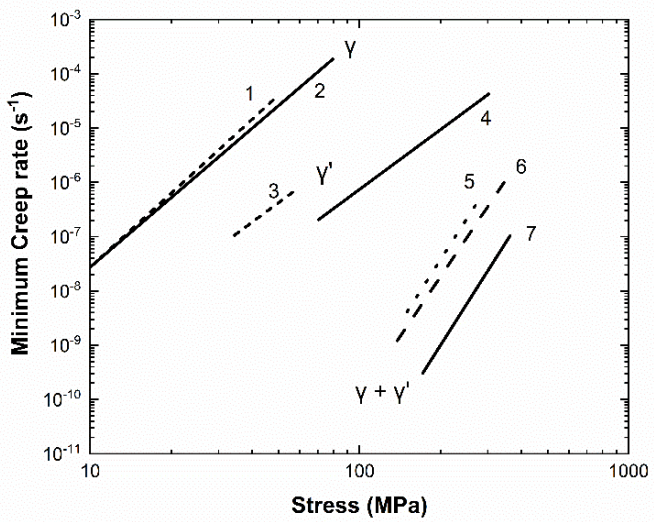

Fig. 2. The minimum creep rates of the γ, γ′, and γ/γ′ structures in Ni-based alloys [12].

Table 1. Chemical compositions and microstructure of the Ni-based alloys in Fig. 2 [13-18].

Label	Chemical composition	Type of microstructure
1	Ni-2W (wt%)	γ
2	Ni-26.5Cr-4.4Al-3.3W-0.6Mo-18.3Co (at%)	γ
3	Ni-12.4Al (wt%)	γ′
4	Ni-2.2Cr-18.8Al-2.4Ti-1.7Ta-1.5W-5.7Co (at%)	γ′
5	Ni-5.78Al-1.22Ti-10.14W-1.09Mo-8.5Cr-3.3Ta (wt%)	γ + γ′
6	Ni-3.7Al-4.2Ti-4Ta-0.5Nb-6W-1.5Mo-9Cr-7.5Co (wt%)	γ + γ′
7	Ni-6Al-4.5Cr-12.5Co-0.16Hf-6.3Re-7Ta-5.8W (wt%)	γ + γ′

2.2. Grain structure

To obtained enhanced creep properties, the grain structure of Ni-based superalloys has been developed from equiaxed-grained to columnar-grained and to single crystal structures. In the early days, superalloys were fabricated via a wrought and conventional casting method, so the appearance of grain boundaries in these superalloys are inevitable [22]. Due to the grain-boundary sliding and the formation of shrinkage porosity at high temperatures, the equiaxed-grained superalloys is difficult to achieve a desired creep performance [23]. To reduce the detrimental effects of grain boundaries at high temperatures, two major strategies have been developed. The first strategy is to introduce stable carbides to the grain boundaries for inhibiting the grain-boundary sliding and enhancing the creep resistance, but the benefits are limited [22]. The second strategy is to eliminate the formation of grain boundaries by preparing single-crystal superalloys, which is used for fabricating turbine blades at the present time. The creep curves of the Mar-M200 superalloys with equiaxed-grained, columnar-grained, and single-crystal structures are shown in Fig. 3. The single-crystal superalloy achieves much better creep performance than the columnar-grained and equiaxed-grained superalloys.

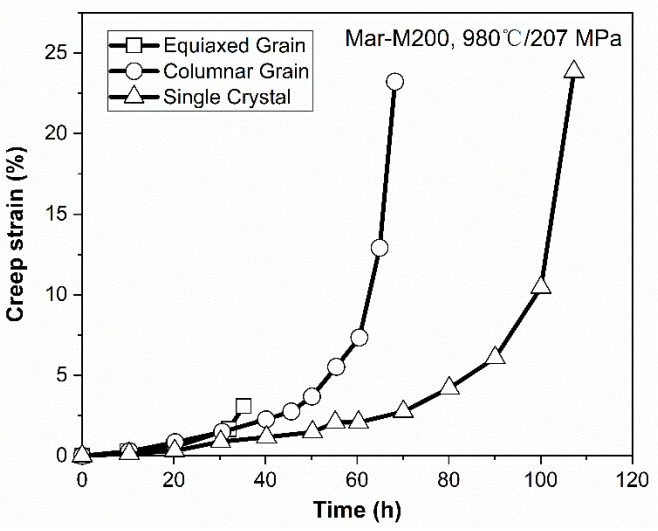

Fig. 3. Creep curves of the Mar-M200 superalloys with equiaxed grains, columnar grains and single crystals [10].

3. Chemical composition and alloying effects

The intrinsic parameters, such as lattice misfit, elastic properties, stacking fault energy of γ matrix, and APB energy of γ′ precipitates are very sensitive to the alloy composition, and alloying additions play an important role in controlling the high-temperature properties of superalloys. In the

following section, the effects of alloying elements on the microstructure and mechanical properties of Ni-based superalloys are briefly reviewed.

(1) γ′-forming element

The γ′-forming elements, such as Ti and Ta, prefer to partition to the γ′ precipitates and occupy the Al sublattice. Adding γ′-forming elements to Ni-based superalloys can influence the strengthening effect by affecting the intrinsic properties of the γ′ phase, such as the APB energy. Generally, the dislocations move into the $L1_2$-ordered γ′ phase by forming APB with the Burger′s vector of a<110>, while the dislocations in the γ phase travel across the matrix with the formation of stacking faults with the Burger′s vector of a/2<110> [24]. The increased length of the Burger's vector indicates that a full dislocation in the γ′ phase is equivalent to two full dislocations in the γ phase. In addition, the APB energy of Ni_3Al is 172 mJ/m^2 [25], higher than the intrinsic stacking fault energy of Ni (121 mJ/m^2) [26]. High APB energy hinders the movement of dislocations in the Ni_3Al-type γ′ phase. Therefore, the slip deformation in the Ni-based γ′ phase is more difficult than that in the γ phase, contributing to the strengthening effect of the γ′ phase. The effects of Ti on the APB energy of Ni-based superalloys are shown in Fig. 4a [11]. The Ti additions monotonically improve the APB energy, contributing to a high stress rupture life [27]. However, excessive Ti additions may lead to the coarsening of γ′ phase and the formation of Ni_3Ti, which deteriorates the mechanical properties of superalloys [28, 29]. Figure 4b shows the effect of Ta on the APB energy of $Ni_3Al_{(1-x)}Ta_x$ alloys [11]. The APB energy increases with the increased Ta/Al ratio and reaches a peak of approximate 600 mJ/m^2 at the Ta/Al ratio of 0.2. Ta is more effective than Ti in improving the APB energy of γ′ phase. Experimental observations also show that Ta has a higher strengthening effect than Ti [30].

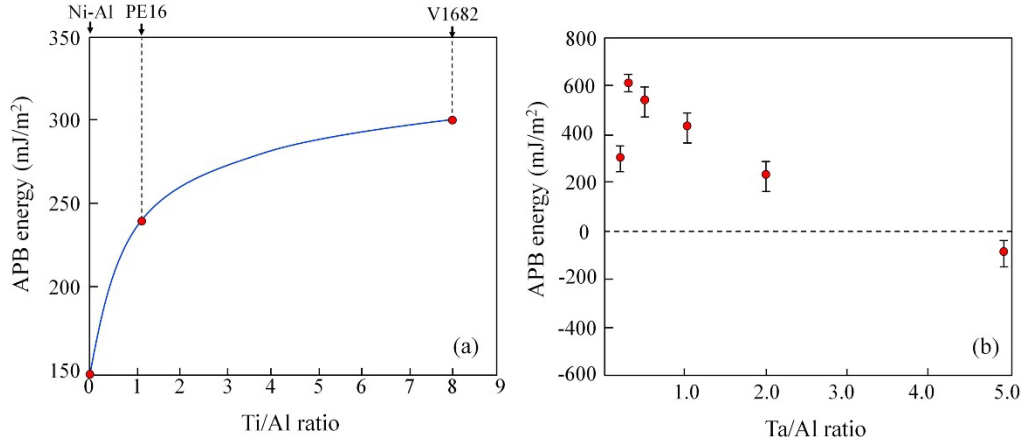

Fig. 4. (a) Effect of Ti on the APB energy of Ni-based superalloys as a function of Ti/Al ratio, and (b) effect of Ti on the APB energy of $Ni_3Al_{(1-x)}Ta_x$ alloys as a function of Ta/Al ratio.

(2) γ-forming element

The γ-forminng elements, such as Cr, Co, Mo, W, Re, and Ru, prefer to partition to the γ matrix, which improve the mechanical properties of Ni-based superalloys by inducing solid solution strengthening, decreasing the stacking fault energy, increasing melting temperatures, and/or decreasing diffusion rate [9, 31, 32].

As for the solid solution strengthening, solute elements with larger atomic sizes than Ni can induce the lattice misfit and/or change the elastic modulus, increasing the resistance to the dislocation movement and improving the mechanical strength [33, 34]. The effects of lattice misfit

and elastic modulus on the solid solution strengthening of Ni-based superalloys are shown in Fig. 5 [35]. The change of lattice misfit and elastic modulus can be obtained by evaluating the volumes and moduli of Ni-based alloys with different alloying additions. Figure 5a shows the shear modulus of Ni-based superalloys decreases linearly with the increased volume, indicating that the change of shear modulus strongly correlates with the lattice misfit. Figure 5b reveals that the 0.2% flow stress increases with the decreasing of the Young's modulus. Considering that the Young's modulus and shear modulus have an near-linear relationship in Ni-based superalloys, the change of lattice misfit by adding large solute elements in Ni dominate the solid-solution strengthening effect [35].

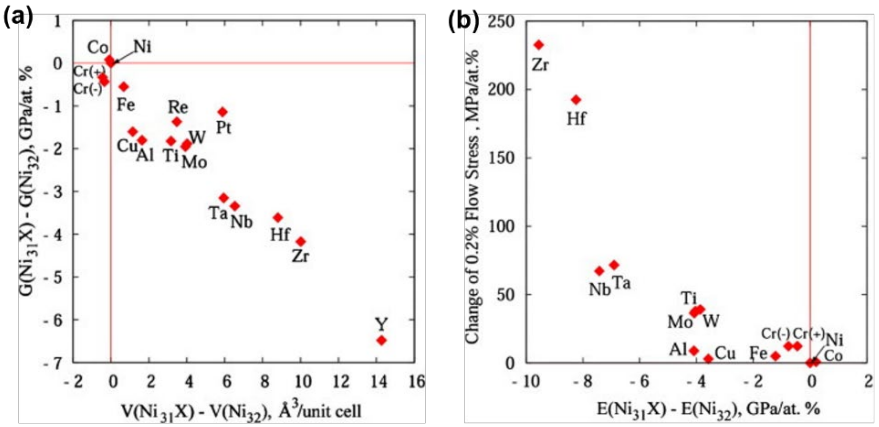

Fig. 5. Effects of lattice misfit and elastic modulus on the solid-solution strengthening of Ni-based superalloys: (a) the relationship between shear modulus (G) and volume (V) and (b) the relationship between Young's modulus (E) and 0.2% flow stress [35].

In the γ matrix, a full dislocation $a/2<1\ 1\ 0>$ is decomposed into two partial dislocations, which are separated by a stacking fault width. This process can be expressed as $a/2[\bar{1}10] \rightarrow a/6[\bar{1}2\bar{1}] + a/6[\bar{2}11]$ [36]. The stacking fault energy can be described as the additional energy required for the formation of a partial dislocation of unit area. A small stacking fault energy contributes to a large stacking fault width, restraining the movement of dislocations in the γ matrix so as to improve the creep strength of alloys [37, 38]. The evolution of the stacking fault energy with solute concentration in dilute Ni–X alloys is summarized in Fig. 6 [39]. The results indicate that the γ-forming elements, including Cr, Co, Mo, W, Re, and Ru, decrease the stacking fault energies of dilute Ni–X alloys with the increased solute concentration. In addition to the theoretical calculations [40], experimental measurements also reported similar findings [41, 42].

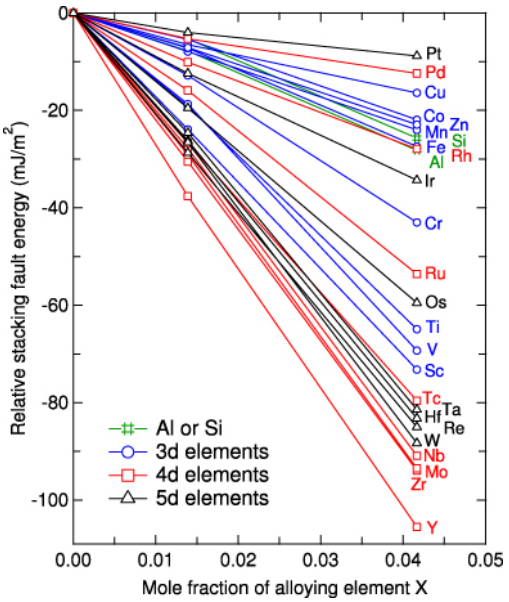

Fig. 6. Calculated stacking fault energy of dilute Ni–X alloys with reference to the pure Ni at 0 K [39].

Considering that Ni-based superalloys are frequently employed in aggressive service environments at high temperatures for long-term periods, a high melting temperature is required for maintaining the high thermal stability and mechanical properties [43, 44]. It is crucial to add certain amounts of refractory elements, such as Co, Re, W, and Ru, to improve the solidus and liquidus lines of Ni-based superalloys. The solidus and liquidus lines of Ni-X binary alloys with different contents of alloying elements are shown in Fig. 7 [11]. The results show that W, Co, Ru, and Re can increase solidus and liquidus temperature, while Mo and Cr lead to an opposite trend. In addition, the concentration of alloying elements should be controlled. For example, the maximum concentrations of Mo and Cr in the Ni-based superalloys are 12.3 and 26.5 at.%, respectively [11].

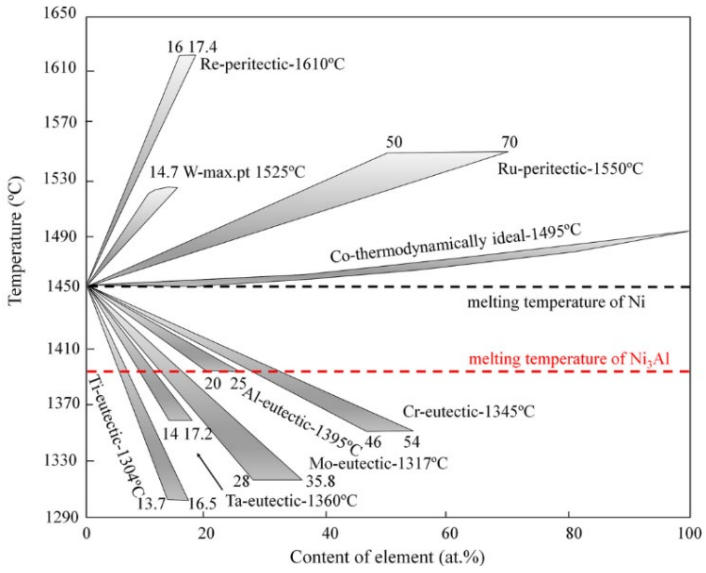

Fig. 7. The solidus and liquidus lines of Ni-X binary alloys with different contents of elements [11]

Solute diffusion plays an important role in controlling the strength and creep resistance of Ni-based superalloys. On the one hand, solute elements can influence the coarsening rate of γ′ precipitates in the γ matrix. Figure 8 shows the coarsening rate constant of γ′ precipitates in different Ni-based superalloys at 1000 ℃ [45]. Re and Ru significantly decrease the coarsening rate constant, while Co promotes the precipitate coarsening rate. Because the diffusion coefficient of Re and Ru is smaller than that of Co in the γ matrix, the low diffusion coefficient hinders the coarsening of γ′ precipitates, thereby improving the creep resistance [9, 46]. On the other hand, the solute elements with a low diffusion coefficient exhibit a high melting temperature, as shown in Fig. 8(b) [44]. Generally, the refractory metals with high melting temperatures, such as W and Mo, have a significant impact in slowing down the coarsening kinetics and improving the mechanical strength [41, 47].

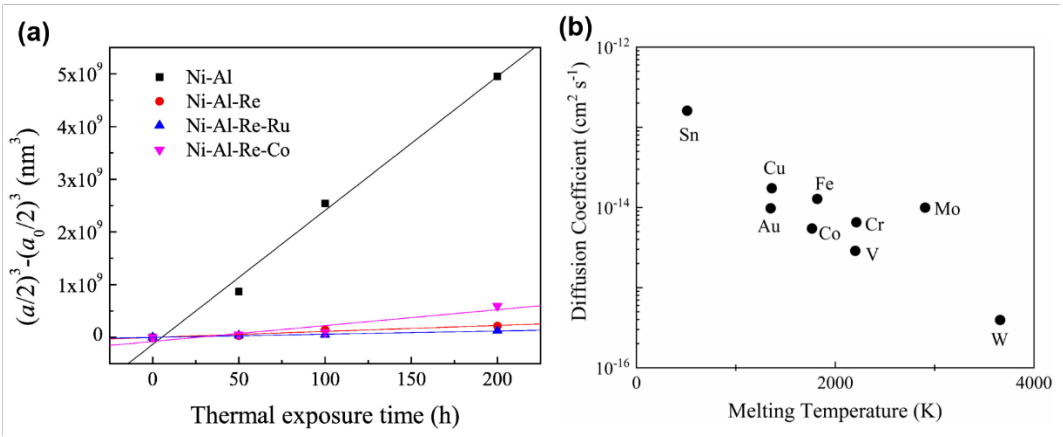

Fig. 8. (a) The coarsening rate constant of γ′ precipitates in Ni-based alloys at 1000 ℃ [45], and (b) the relationship between the diffusion coefficient of elements in Ni at 727 ℃ and their melting temperature [44].

(3) Re effect

Re plays a critical role in controlling the creep performance of Ni-based superalloys [48]. For example, the creep rupture life of third-generation superalloys with 4 at.% Re is approximate 180 h at 1010 ℃ under 248 MPa, while that of the Re-free superalloys is just 20 h [49]. Although extensive efforts have been made to study the origin of Re effects on mechanical properties, the conclusive understanding is still incomplete.

In the early days, good creep resistance was obtained by doping Re in the first-generation superalloys of CMSX-2 and PWA-1480 [50]. One explanation is that the Re clusters exist in the γ matrix, which act as strong obstacles to hinder the movement of dislocations [51]. For validating the mechanism, experimental and theoretical studies have been performed, but some results contradict each other. For example, Rüsing *et al*. [52] found that Re can form clusters with the size of approximately 1 nm in the Ni-Al-Ta-Re alloys by using three-dimensional atom probe tomography. However, no Re cluster was found in the binary Ni-Re system by analyzing the X-ray absorption data [53]. Theoretically, Zhu *et al*. [54] showed that Re atoms have a tendency to form clusters in both the γ and γ′ phases by using molecular dynamics calculations. This contradicts the findings of by Mottura et al, who reported that the Re-Re nearest neighbor pair has a strong repulsion [55]. Therefore, the formation of Re clusters may be related to the other solute elements

in Ni-based superalloys, which needs further investigation. In addition, in-situ observations of dislocation motion around the Re clusters provide important evidence for revealing the effect of Re clusters on the creep resistance of Ni-based superalloys.

The second effect of Re on improving the mechanical properties of Ni-based superalloys is attributed to the co-segregation of Re with other alloying elements at the γ/γ′ interface. Figure 9. shows the dislocation structure and elemental distribution at the γ/γ′ interface [56]. The EDS mapping provides the evidence for the co-segregation of Re with Cr, Co, and Mo at the γ/γ′ interface. This phenomenon also provides indirect evidence that other solute elements may contribute to the formation of the Re clusters. This co-segregation can pin dislocations at the γ/γ′ interface, thereby hindering the dislocation motion.

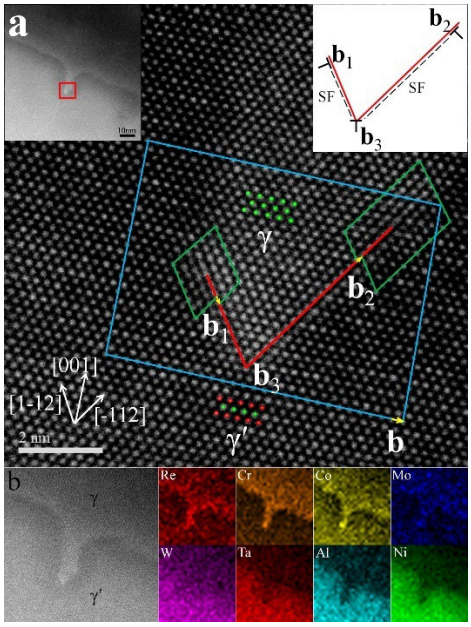

Fig. 9. (a) High resolution HAADF-STEM image of the dislocation core structure at the γ/γ′ interface. (b) Elemental distribution map at the γ/γ′ interface [56].

The low diffusion rate of Re in the γ matrix influences the creep behavior of Ni-based superalloys. The diffusion coefficients of some refractory elements (Ta, W, and Re) in Ni at different temperatures is shown in Fig. 10 [57]. It it evident that Re has the slowest diffusion rate among the three elements [57]. First-principles calculations indicate that the slow diffusion rate of Re is due to the bonding characteristics of the *d* electrons [58]. The slow diffusing of Re can influence the vacancy diffusion in γ matrix, slowing down the dislocation motion and improving creep resistance at high temperatures [59]. In addition, Re also has solid solution strengthening effect, which originates from a larger atomic size of Re than that of Ni [9].

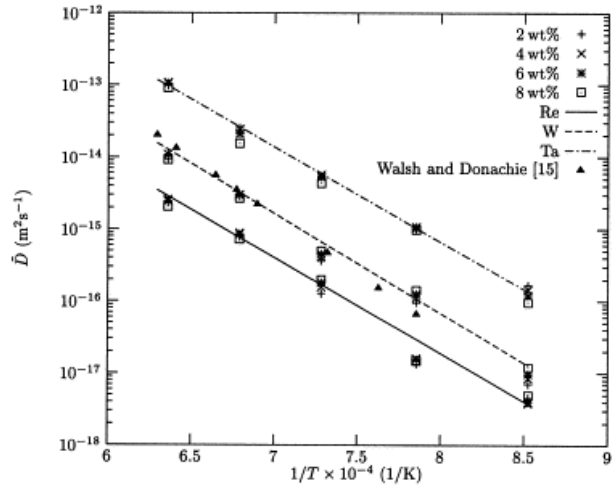

Fig. 10. Diffusion coefficients of Ta, W, and Re in Ni at different temperatures [57].

(4) Ru effect

Excessive Cr, Re, W, and Mo additions lead to the formation of topologically closed packed (TCP) phases, which have detrimental effects on the high-temperature performance of Ni-based superalloys [60]. On the one hand, the formation of TPC phases consumes refractory elements in the γ matrix, decreasing solid-solution strengthening effect. On the other hand, the TCP phases are brittle. Irregular TCP phases in the γ matrix causes a large stress concentration, which is likely to serve as the site for microcrack initiation and propagation. Thus, controlling the distribution and composition of TCP phases are very important for the design of high-performance superalloys. Intriguingly, Ru additions have been found to suppress the formation of TCP phases [61]. To reveal the underlying mechanisms of the Ru effect, extensive attempts have been made. One important finding is that Ru additions reduces the partitioning of refractory elements to the γ matrix, which is also called reverse partitioning [62, 63]. Figure 11a compares the partition ratios of Cr, Mo, W, and Re in the Ni-based superalloys without and with Ru additions, denoted as 0Ru and 3Ru, respectively [63]. The addition of 3% Ru in the Ni-based superalloys significantly reduces the partition ratio of Re. Thus, the reduced Re concertation in the γ matrix inhibits the formation of TCP phases, as shown in Figs. 11b and c. However, no such reverse partitioning behavior is observed in some superalloys containing Ru, while the effect of inhibiting the formation of TCP phases still exists [64]. Thus, another possibility for the inhibition of TCP phases is that the Ru addition increases the lattice misfit between the TCP phase and γ matrix, leading to an increased elastic strain energy and hence raising the energy barrier for the nucleation of TCP phases [65].

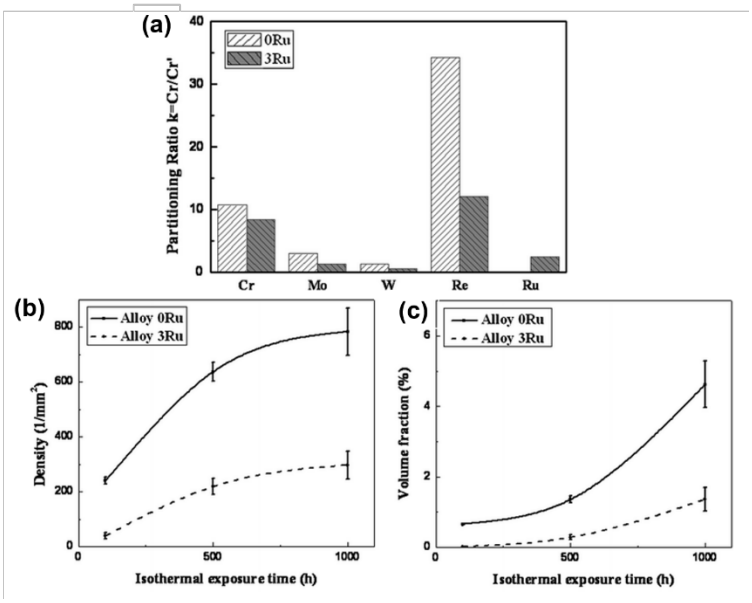

Fig. 11. (a) Partitioning ratios of alloying elements and (b) density and (c) volume fraction of TCP precipitates as a function of time in the Ni-based single-crystal superalloys with and without Ru additions [63].

(5) Evolution from the 1st to the 6th generation Ni-based single-crystal superalloys

Ni-based single-crystal superalloys have been developed from the 1st to the 6th generation, and the temperature capabilities have increased from 1000 to 1120 ℃. The development of high temperature performance cannot be realized without the progress of alloy design. The chemical compositions of some typical Ni-based superalloys from the 1st to the 6th generation are shown in Table 2 [66]. The 1st generation Ni-based single crystalline superalloys mainly contain Ni, Cr, Mo, W, Co, Al, Ti, and Ta. Considering the strengthening effect of Re on the creep properties, 3 wt.% Re was added to the 2nd generation, and the service temperature increases by about 30 °C [67]. In the 3rd generation, the Re content further increases to about 5 wt.%. However, excess Re additions lead to the formation of TCP phases, which have detrimental effect on the mechanical properties of Ni-based superalloys. To hinder the formation of TCP phases, 2 wt.% Ru was added in the 4th generation. In the latest 5th and 6th generations, the Ru content increases to above 5 wt.%. Considering the possibilities of synthetic effects between Ru, Re and other elements in the Ni-based superalloys, chemical compositions still have a lot of space to explore.

Table 2. Chemical compositions of some typical Ni-based superalloys from the 1st to the 6th generation (wt%) [66].

Generation	Alloy	Ni	Co	Cr	Mo	W	Al	Ti	Ta	Re	Ru
1st	CMSX-2	Bal.	4.6	8.0	0.6	8.0	5.6	1.0	9.2	-	-
	PWA1480	Bal.	5.0	10.0	-	4.0	5.0	1.5	12	-	-
	SRR99	Bal.	5.0	8.0	-	10.0	5.5	2.2	3.0	-	-
2nd	CMSX-4	Bal.	9.0	6.5	0.6	6.0	5.6	1.0	6.5	3.0	-
	Rene N5	Bal.	8.0	7.0	2.0	5.0	6.2	-	7.0	3.0	-
	PWA1484	Bal.	10.0	5.0	2.0	6.0	5.6	-	9.0	3.0	-
3rd	TMS-75	Bal.	12.0	3.0	2.0	6.0	6.0-	-	6.0	5.0	-
	CMSX-10	Bal.	3.0	2.0	0.4	5.0	5.7	0.2	8.0	6.0	-
	Rene N6	Bal.	12.5	4.2	1.4	6.0	5.7	-	7.2	5.4	-
4th	PWA1497	Bal.	16.5	2.0	2.0	6.0	5.5	-	8.2	5.9	3.0

	MC-NG	Bal.	-	4.0	5.0	1.0	6.0	0.5	5.0	4.0	4.0
	TMS-138	Bal.	5.8	3.2	2.9	5.9	5.8	-	5.6	5.0	2.0
5th	TMS-162	Bal.	5.8	3.0	3.9	5.8	5.8	-	5.6	4.9	6.0
	TMS-196	Bal.	5.6	4.6	2.4	5.0	5.6	-	5.6	6.4	5.0
6th	TMS-238	Bal.	6.5	4.6	1.1	4.0	5.9	-	7.6	6.4	5.0

4. Thermal stability and Creep performance

(1) Evolution of γ/γ′ microstructure in the three stages of creep process

The creep resistance and high-temperature strength of Ni-based superalloys are closely related to the dislocation motion and evolution of the γ′/γ microstructure [68, 69]. Generally, the creep curves are divided into three stages, and the creep rate can be used for evaluating the creep resistance, as shown in Fig. 12. In the primary creep stage, dislocations start to multiply in the γ channels and at the γ/γ′ interface, leading to the high creep rate at the beginning of this creep stage [70]. With the enhancement of dislocation activities, dense dislocation networks at the γ/γ′ interface gradually suppress the movements of dislocations. At the end of the primary creep stage, the creep rate decreases to a minimum value. In this stage, the γ/γ′ interface is regular. During the second creep stage, the creep rate reaches a balanced state and keeps a constant rate until the end of this stage. Considering the low creep rate among the creep processes, this stage accounts for most of the creep life. In this stage, the dislocation networks around raft γ′ precipitates increases in number and gradually reaches a steady state [71]. In the tertiary creep stage, the creep rate starts to increase due to the degenerate of the γ/γ′ microstructure, and finally the creep rupture occurs [72].

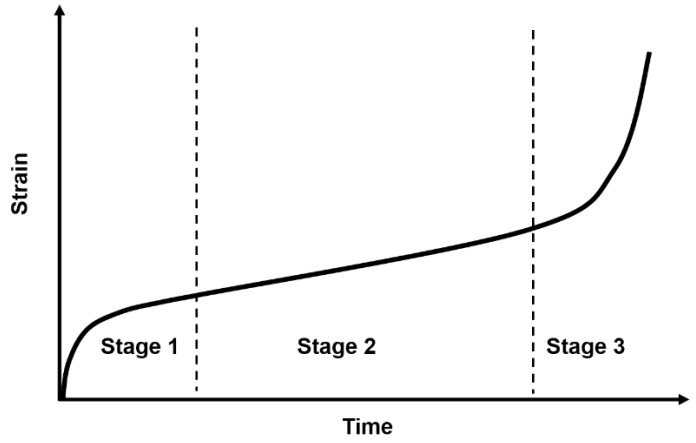

Fig. 12. Schematic diagram of strain as a function of time under constant temperature and stress during creep process.

(2) Volume fraction of γ′ phase

The γ′ phase acts as a barrier to prevent dislocations from penetrating during the creep deformation. Under moderate temperatures and stresses, the increased volume fraction of γ′ phase with optimized structures makes dislocations overcome the γ′ phase by Orowan bowing, and this significantly enhances the creep resistance [73]. In addition, experimental observation has shown that the creep resistance of γ′ structure is higher than that of γ structure [12]. However, excessive γ′ phases reduce the creep rupture life [74]. This is because the γ channels provide sites for the formation of dense dislocation microstructures, which inhibits the dislocation motion [75]. More γ′ phases lead to the less and thinner γ channels. Consequently, controlling a suitable range of volume

fractions of γ′ is very important to obtain excellent creep resistance.

The relationship between the creep rupture life and volume fraction of γ′ phase in two Ni-based superalloys is shown Fig. 13 [76]. First, the volume fraction of γ′ phase with the longest creep rupture life is temperature-dependent. The γ′ volume fraction with the longest rupture life is 70% at 900 ˚C and 55% at 1100 ˚C. Second, alloy compositions also influence the γ′ volume fraction with the longest rupture life. At 900 ˚C, the creep performance of the TMS-75 superalloy is superior to that of the TMS-82+ superalloy at all of the γ′ volume fractions. Anyhow, the volume fraction of γ′ phase should be controlled in an appropriate range, generally from 50% to 70% for single-crystal superalloys [77].

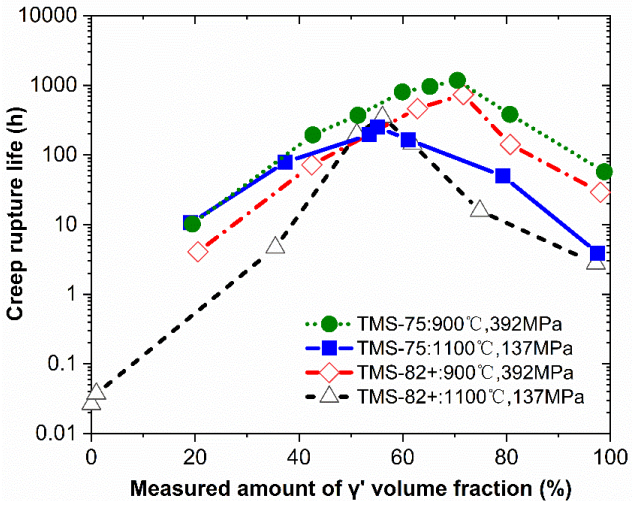

Fig. 13. Influences of γ′ volume fraction on creep rupture life in two Ni-based superalloys [76].

(3) Size and shape of γ′ precipitates

The size and shape of γ′ precipitate play an important role in controlling the creep resistance. The relationships between the creep rupture life and the size and shape of the initial γ′ precipitates are shown in Fig. 14 [78]. Three precipitate morphologies are considered, including the spherical, cubic and irregular raft structures. It is evident that the shape of γ′ precipitates evolves from spherical to cuboidal and to irregular raft shape during the coarsening of γ′ precipitates. This transition of morphology depends highly on the coherency strain, which is associated with the lattice misfit between the γ′ and γ phases [77]. The γ′ precipitates with a cuboidal shape exhibit the highest creep life among all morphologies, and the optimal initial size of the cuboids is 0.35~0.45 mm. The control of size and shape of γ′ precipitates can be achieved by the optimization of heat treatments [79, 80].

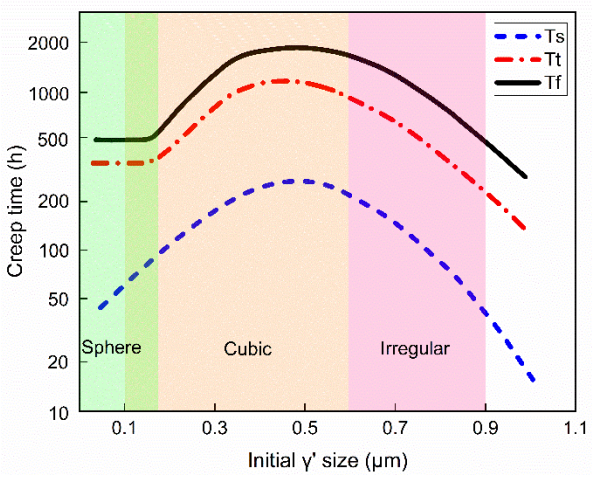

Fig. 14. Relationship between the creep properties and initial γ′ size. The symbol of Ts, Tt, and Tf denote the time to the start of secondary creep stage, the time to the start of tertiary creep stage, and the time to failure, respectively [78].

5. Summary

The fundamental understanding of the effect of alloying elements on the intrinsic parameters, microstructures, and mechanical properties is essential for the design of advanced Ni-based superalloys. The major characteristics are summarized as follows:

1. The Ni-based superalloys consist of Ni-type γ phase and Ni_3Al-type and γ′ phase. The γ′ precipitates are coherent with the continuous γ matrix in the form of cuboidal shape. The dual-phase structure exhibits more effective creep resistance than the single-phase one, which is due to dense dislocation networks at the γ/γ′ interface. Grain boundary has detrimental effects on the high-temperature performance, and single-crystal superalloys can achieve superior creep resistance.
2. Ti and Ta prefer to partitioning into the γ′ precipitates. Adding small amounts of Ti and Ta to the γ′ phase significantly increases the APB energy. A high APB energy contributes to inhibiting the motion of dislocations in γ′ phase, thereby enhancing the strengthening effect.
3. Cr, Co, Mo, and W prefer to partitioning into the γ matrix. The main contributions of these solutes to the strengthening can be threefold. First, the misfit between these solutes and the γ matrix dominates the solid solution strengthening. Second, the stacking fault energy decreases with additions of these alloying elements, leading to a larger stacking fault width and hence restraining the dislocation motion in the γ matrix. Third, the low diffusivity of solutes inhibits the coarsening of γ′ precipitates.
4. Re has a strong tendency to partition to the γ matrix. Re plays a more effective role in the creep performance than Cr, Co, Mo, and W, while the strengthening mechanisms are still under debate. There are two popular viewpoints. One is that the Re clusters form within the γ matrix, which act as strong obstacles to hinder the movement of dislocations. The other is that the co-segregation of Re with other alloying elements at the γ/γ′ interface contribute to the pinning of dislocations at the γ/γ′ interface, thereby hindering the dislocation motion. In addition, the Re effect is also related to other mechanisms, such as the solid-solution strengthening and low diffusivity.
5. Excessive Cr, Re, W, and Mo additions lead to the formation of TCP phases, which have

detrimental effects on the high-temperature performance. Ru prefers to segregate into the γ matrix, which significantly suppresses the formation of TCP phases. Two possible mechanisms are used to explain the phenomena. The first is that the Ru additions significantly reduce the partitioning ratio of Re in the γ matrix, inhibiting the formation of TCP phases. However, in some Ru-containing superalloys, the γ matrix can contain a high Re content, while the formation of TCP phases is still inhibited. A possible explanation is that Ru increases the lattice misfit between the TCP phase and γ matrix, leading to an increased elastic strain energy and hence raiseing the energy barrier for the nucleation of TCP phases.

6. The microstructure parameters, including the volume fraction, size, and shape of γ′ phases, play an important role in controlling the high-temperature performance. The volume fraction of γ′ phase should be controlled in an appropriate range, generally from 50% to 70% for single-crystal superalloys, and the optimal initial size of the γ′ cuboids is 0.35~0.45 mm.

References

[1] P.J. Blau, T.M. Brummett, B.A. Pint, Effects of prior surface damage on high-temperature oxidation of Fe-, Ni-, and Co-based alloys, Wear 267(1) (2009) 380-386.

[2] K.O. Findley, J.L. Evans, A. Saxena, A critical assessment of fatigue crack nucleation and growth models for Ni- and Ni,Fe-based superalloys, International Materials Reviews 56(1) (2011) 49-71.

[3] L. Thivillon, P. Bertrand, B. Laget, I. Smurov, Potential of direct metal deposition technology for manufacturing thick functionally graded coatings and parts for reactors components, Journal of Nuclear Materials 385(2) (2009) 236-241.

[4] L. Luo, Y. Ma, S. Li, Y. Pei, L. Qin, S. Gong, Evolutions of microstructure and lattice misfit in a γ′-rich Ni-based superalloy during ultra-high temperature thermal cycle, Intermetallics 99 (2018) 18-26.

[5] Ł. Rakoczy, B. Rutkowski, M. Grudzień-Rakoczy, R. Cygan, W. Ratuszek, A. Zielińska-Lipiec, Analysis of γ′ Precipitates, Carbides and Nano-Borides in Heat-Treated Ni-Based Superalloy Using SEM, STEM-EDX, and HRSTEM, Materials 13(19) (2020).

[6] R. Verma, G. Kaushal, High temperature oxidation behavior and characterization of DMLS fabricated Ni based superalloys, Materials Today: Proceedings (2022).

[7] G.R. Thellaputta, P.S. Chandra, C.S.P. Rao, Machinability of Nickel Based Superalloys: A Review, Materials Today: Proceedings 4(2, Part A) (2017) 3712-3721.

[8] J.Z. Zhu, T. Wang, A.J. Ardell, S.H. Zhou, Z.K. Liu, L.Q. Chen, Three-dimensional phase-field simulations of coarsening kinetics of γ′ particles in binary Ni–Al alloys, Acta Materialia 52(9) (2004) 2837-2845.

[9] Q. Ding, S. Li, L.-Q. Chen, X. Han, Z. Zhang, Q. Yu, J. Li, Re segregation at interfacial dislocation network in a nickel-based superalloy, Acta Materialia 154 (2018) 137-146.

[10] N. Das, Advances in nickel-based cast superalloys, Transactions of the Indian Institute of Metals 63(2) (2010) 265-274.

[11] H. Long, S. Mao, Y. Liu, Z. Zhang, X. Han, Microstructural and compositional design of Ni-based single crystalline superalloys — A review, Journal of Alloys and Compounds 743 (2018) 203-220.

[12] T.M. Pollock, R.D. Field, Chapter 63 Dislocations and high-temperature plastic deformation of superalloy single crystals, in: F.R.N. Nabarro, M.S. Duesbery (Eds.), Dislocations in Solids,

Elsevier2002, pp. 547-618.
[13] R.V. Miner, T.P. Gabb, J. Gayda, K.J. Hemker, Orientation and temperature dependence of some mechanical properties of the single-crystal nickel-base superalloy René N4: Part III. Tension-compression anisotropy, Metallurgical Transactions A 17(3) (1986) 507-512.
[14] G. Xiping, F. Hengzhi, Stress Rupture Behaviour of the Single Crystal Superalloy NASAIR 100 at 1050 °C, International Journal of Materials Research 87(4) (1996) 315-320.
[15] T.M. Pollock, The growth and elevated temperature stability of high refractory nickel-base single crystals, Materials Science and Engineering: B 32(3) (1995) 255-266.
[16] W.R. Johnson, C.R. Barrett, W.D. Nix, The high-temperature creep behavior of nickel-rich Ni-W solid solutions, Metallurgical and Materials Transactions B 3(4) (1972) 963-969.
[17] D.M. Shah, Orientation dependence of creep behavior of single crystal γ′ (Ni3Al), Scripta Metallurgica 17(8) (1983) 997-1002.
[18] M.V. Nathal, L.J. Ebert, The influence of cobalt, tantalum, and tungsten on the microstructure of single crystal nickel-base superalloys, Metallurgical Transactions A 16(10) (1985) 1849-1862.
[19] J.X. Zhang, T. Murakumo, H. Harada, Y. Koizumi, Dependence of creep strength on the interfacial dislocations in a fourth generation SC superalloy TMS-138, Scripta Materialia 48(3) (2003) 287-293.
[20] X.G. Liu, L. Wang, L.H. Lou, J. Zhang, Effect of Mo Addition on Microstructural Characteristics in a Re-containing Single Crystal Superalloy, Journal of Materials Science & Technology 31(2) (2015) 143-147.
[21] X.P. Tan, J.L. Liu, T. Jin, Z.Q. Hu, H.U. Hong, B.G. Choi, I.S. Kim, C.Y. Jo, D. Mangelinck, Effect of Ru additions on very high temperature creep properties of a single crystal Ni-based superalloy, Materials Science and Engineering: A 580 (2013) 21-35.
[22] W. Betteridge, S.W.K. Shaw, Development of superalloys, Materials Science and Technology 3(9) (1987) 682-694.
[23] A.F. Giamei, Development of Single Crystal Superalloys: A Brief History, Advanced Materials & Processes 171(9) (2013).
[24] H. Long, Y. Liu, D. Kong, H. Wei, Y. Chen, S. Mao, Shearing mechanisms of stacking fault and anti-phase-boundary forming dislocation pairs in the γ′ phase in Ni-based single crystal superalloy, Journal of Alloys and Compounds 724 (2017) 287-295.
[25] Y. Rao, T.M. Smith, M.J. Mills, M. Ghazisaeidi, Segregation of alloying elements to planar faults in γ'-Ni3Al, Acta Materialia 148 (2018) 173-184.
[26] A. Datta, U.V. Waghmare, U. Ramamurty, Density functional theory study on stacking faults and twinning in Ni nanofilms, Scripta Materialia 60(2) (2009) 124-127.
[27] L. Liu, T. Jin, H. Chen, X. Sun, H. Guan, Z. Hu, Effect of Ti/Al Ratio on the Microstructure and Stress Rupture Property in a Ni-Base Single Crystal Superalloy, Rare Metal Materials and Engineering 38 (2009) 612-616.
[28] M. Tan, C. Wang, Y. Guo, J. Guo, L. Zhou, Influence of Ti/Al ratios on γ' coarsening behavior and tensile properties of GH984G alloy during long-term thermal exposure, Acta Metallurgica Sinica 50 (2014) 1260-1268.
[29] X.B. Hu, X.W. Guo, Y.J. Wang, J.S. Hou, X.Z. Qin, L.Z. Zhou, J.F. Liu, X.L. Ma, Microstructural characterization of the η-Ni3(Ti, Al) phase in a long-term-aged Ni-based superalloy, Philosophical Magazine Letters 97(11) (2017) 442-449.
[30] R. Eriş, M.V. Akdeniz, A.O. Mekhrabov, Atomic size effect of alloying elements on the formation,

evolution and strengthening of γ′-Ni3Al precipitates in Ni-based superalloys, Intermetallics 109 (2019) 37-47.
[31] C. Tian, G. Han, C. Cui, X. Sun, Effects of stacking fault energy on the creep behaviors of Ni-base superalloy, Materials & Design 64 (2014) 316-323.
[32] T. Gaag, N. Ritter, A. Peters, N. Volz, D. Gruber, S. Neumeier, C. Zenk, C. Körner, Improving the Effectiveness of the Solid-Solution-Strengthening Elements Mo, Re, Ru and W in Single-Crystalline Nickel-Based Superalloys, Metals 11(11) (2021).
[33] C. Gui, A. Sato, Y. Gu, H. Harada, Microstructure and yield strength of UDIMET 720LI alloyed with Co-16.9 Wt Pct Ti, Metallurgical and Materials Transactions A 36(11) (2005) 2921-2927.
[34] M.V. Nathal, R.D. Maier, L.J. Ebert, The Influence of Cobalt on the Microstructure of the Nickel-Base Superalloy MAR-M247, Metallurgical Transactions A 13(10) (1982) 1775-1783.
[35] D. Kim, S.-L. Shang, Z.-K. Liu, Effects of alloying elements on elastic properties of Ni by first-principles calculations, Computational Materials Science 47(1) (2009) 254-260.
[36] S.L. Shang, W.Y. Wang, Y. Wang, Y. Du, J.X. Zhang, A.D. Patel, Z.K. Liu, Temperature-dependent ideal strength and stacking fault energy of fcc Ni: a first-principles study of shear deformation, Journal of Physics: Condensed Matter 24(15) (2012) 155402.
[37] M. Huang, Z. Li, The key role of dislocation dissociation in the plastic behaviour of single crystal nickel-based superalloy with low stacking fault energy: Three-dimensional discrete dislocation dynamics modelling, Journal of the Mechanics and Physics of Solids 61(12) (2013) 2454-2472.
[38] C.P. Liu, X.N. Zhang, L. Ge, S.H. Liu, C.Y. Wang, T. Yu, Y.F. Zhang, Z. Zhang, Effect of rhenium and ruthenium on the deformation and fracture mechanism in nickel-based model single crystal superalloys during the in-situ tensile at room temperature, Materials Science and Engineering: A 682 (2017) 90-97.
[39] S.L. Shang, C.L. Zacherl, H.Z. Fang, Y. Wang, Y. Du, Z.K. Liu, Effects of alloying element and temperature on the stacking fault energies of dilute Ni-base superalloys, Journal of Physics: Condensed Matter 24(50) (2012) 505403.
[40] X.-X. Yu, C.-Y. Wang, The effect of alloying elements on the dislocation climbing velocity in Ni: A first-principles study, Acta Materialia 57(19) (2009) 5914-5920.
[41] B.E.P. Beeston, I.L. Dillamore, R.E. Smallman, The Stacking-Fault Energy of Some Nickel-Cobalt Alloys, Metal Science Journal 2(1) (1968) 12-14.
[42] Y. Yuan, Y. Gu, C. Cui, T. Osada, Z. Zhong, T. Tetsui, T. Yokokawa, H. Harada, Influence of Co content on stacking fault energy in Ni–Co base disk superalloys, Journal of Materials Research 26(22) (2011) 2833-2837.
[43] K.A. Christofidou, N.G. Jones, E.J. Pickering, R. Flacau, M.C. Hardy, H.J. Stone, The microstructure and hardness of Ni-Co-Al-Ti-Cr quinary alloys, Journal of Alloys and Compounds 688 (2016) 542-552.
[44] A.K. Jena, M.C. Chaturvedi, The role of alloying elements in the design of nickel-base superalloys, Journal of Materials Science 19(10) (1984) 3121-3139.
[45] S. Liu, C. Liu, L. Ge, X. Zhang, T. Yu, P. Yan, C. Wang, Effect of interactions between elements on the diffusion of solutes in NiXY systems and γ′-coarsening in model Ni-based superalloys, Scripta Materialia 138 (2017) 100-104.
[46] X. Zhang, H. Deng, S. Xiao, Z. Zhang, J. Tang, L. Deng, W. Hu, Diffusion of Co, Ru and Re in Ni-based superalloys: A first-principles study, Journal of Alloys and Compounds 588 (2014) 163-

169.
[47] C.E. Campbell, W.J. Boettinger, U.R. Kattner, Development of a diffusion mobility database for Ni-base superalloys, Acta Materialia 50(4) (2002) 775-792.
[48] X. Wu, S.K. Makineni, C.H. Liebscher, G. Dehm, J. Rezaei Mianroodi, P. Shanthraj, B. Svendsen, D. Bürger, G. Eggeler, D. Raabe, B. Gault, Unveiling the Re effect in Ni-based single crystal superalloys, Nature Communications 11(1) (2020) 389.
[49] T. Jin, W.Z. Wang, X.F. Sun, Z.Q. Hu, Role of Rhenium in Single Crystal Ni-Based Superalloys, Materials Science Forum 638-642 (2010) 2257-2262.
[50] D. Blavette, P. Caron, T. Khan, An atom probe investigation of the role of rhenium additions in improving creep resistance of Ni-base superalloys, Scripta Metallurgica 20(10) (1986) 1395-1400.
[51] N. Wanderka, U. Glatzel, Chemical composition measurements of a nickel-base superalloy by atom probe field ion microscopy, Materials Science and Engineering: A 203(1) (1995) 69-74.
[52] J. Rüsing, N. Wanderka, U. Czubayko, V. Naundorf, D. Mukherji, J. Rösler, Rhenium distribution in the matrix and near the particle–matrix interface in a model Ni–Al–Ta–Re superalloy, Scripta Materialia 46(3) (2002) 235-240.
[53] A. Mottura, R.T. Wu, M.W. Finnis, R.C. Reed, A critique of rhenium clustering in Ni–Re alloys using extended X-ray absorption spectroscopy, Acta Materialia 56(11) (2008) 2669-2675.
[54] T. Zhu, C.-y. Wang, Y. Gan, Effect of Re in γ phase, γ′ phase and γ/γ′ interface of Ni-based single-crystal superalloys, Acta Materialia 58(6) (2010) 2045-2055.
[55] A. Mottura, M.W. Finnis, R.C. Reed, On the possibility of rhenium clustering in nickel-based superalloys, Acta Materialia 60(6) (2012) 2866-2872.
[56] M. Huang, Z. Cheng, J. Xiong, J. Li, J. Hu, Z. Liu, J. Zhu, Coupling between Re segregation and γ/γ′ interfacial dislocations during high-temperature, low-stress creep of a nickel-based single-crystal superalloy, Acta Materialia 76 (2014) 294-305.
[57] M.S.A. Karunaratne, P. Carter, R.C. Reed, Interdiffusion in the face-centred cubic phase of the Ni–Re, Ni–Ta and Ni–W systems between 900 and 1300°C, Materials Science and Engineering: A 281(1) (2000) 229-233.
[58] A. Janotti, M. Krčmar, C.L. Fu, R.C. Reed, Solute Diffusion in Metals: Larger Atoms Can Move Faster, Physical Review Letters 92(8) (2004) 085901.
[59] S. Gao, Z. Yang, M. Grabowski, J. Rogal, R. Drautz, A. Hartmaier, Influence of Excess Volumes Induced by Re and W on Dislocation Motion and Creep in Ni-Base Single Crystal Superalloys: A 3D Discrete Dislocation Dynamics Study, Metals 9(6) (2019).
[60] B. Seiser, R. Drautz, D.G. Pettifor, TCP phase predictions in Ni-based superalloys: Structure maps revisited, Acta Materialia 59(2) (2011) 749-763.
[61] A. Sato, H. Harada, T. Yokokawa, T. Murakumo, Y. Koizumi, T. Kobayashi, H. Imai, The effects of ruthenium on the phase stability of fourth generation Ni-base single crystal superalloys, Scripta Materialia 54(9) (2006) 1679-1684.
[62] Z.-x. Shi, J.-r. Li, S.-z. Liu, Effects of Ru on the microstructure and phase stability of a single crystal superalloy, International Journal of Minerals, Metallurgy, and Materials 19(11) (2012) 1004-1009.
[63] X. Tan, J. Liu, T. Jin, Z. Hu, H.U. Hong, B.G. Choi, I.S. Kim, Y.S. Yoo, C.Y. Jo, Effect of Ruthenium on Precipitation Behavior of the Topologically Close-Packed Phase in a Single-Crystal Ni-Based Superalloy During High-Temperature Exposure, Metallurgical and Materials Transactions A 43(10)

(2012) 3608-3614.
[64] R.C. Reed, A.C. Yeh, S. Tin, S.S. Babu, M.K. Miller, Identification of the partitioning characteristics of ruthenium in single crystal superalloys using atom probe tomography, Scripta Materialia 51(4) (2004) 327-331.
[65] Z. Peng, I. Povstugar, K. Matuszewski, R. Rettig, R. Singer, A. Kostka, P.-P. Choi, D. Raabe, Effects of Ru on elemental partitioning and precipitation of topologically close-packed phases in Ni-based superalloys, Scripta Materialia 101 (2015) 44-47.
[66] W. Xia, X. Zhao, L. Yue, Z. Zhang, A review of composition evolution in Ni-based single crystal superalloys, Journal of Materials Science & Technology 44 (2020) 76-95.
[67] P. Caron, T. Khan, Evolution of Ni-based superalloys for single crystal gas turbine blade applications, Aerospace Science and Technology 3(8) (1999) 513-523.
[68] P.M. Sarosi, R. Srinivasan, G.F. Eggeler, M.V. Nathal, M.J. Mills, Observations of a 〈010〉 dislocations during the high-temperature creep of Ni-based superalloy single crystals deformed along the [001] orientation, Acta Materialia 55(7) (2007) 2509-2518.
[69] D. Tytko, P.-P. Choi, J. Klöwer, A. Kostka, G. Inden, D. Raabe, Microstructural evolution of a Ni-based superalloy (617B) at 700°C studied by electron microscopy and atom probe tomography, Acta Materialia 60(4) (2012) 1731-1740.
[70] T. Link, A. Epishin, M. Paulisch, T. May, Topography of semicoherent γ/γ′-interfaces in superalloys: Investigation of the formation mechanism, Materials Science and Engineering: A 528(19) (2011) 6225-6234.
[71] T. Sugui, Z. Huihua, Z. Jinghua, Y. Hongcai, X. Yongbo, H. Zhuangqi, Formation and role of dislocation networks during high temperature creep of a single crystal nickel–base superalloy, Materials Science and Engineering: A 279(1) (2000) 160-165.
[72] Y. Tang, M. Huang, J. Xiong, J. Li, J. Zhu, Evolution of superdislocation structures during tertiary creep of a nickel-based single-crystal superalloy at high temperature and low stress, Acta Materialia 126 (2017) 336-345.
[73] T.B. Gibbons, B.E. Hopkins, Creep behaviour and microstructure of Ni-Cr base alloys, Metal Science 18(5) (1984) 273-280.
[74] T. Murakumo, T. Kobayashi, Y. Koizumi, H. Harada, Creep behaviour of Ni-base single-crystal superalloys with various γ′ volume fraction, Acta Materialia 52(12) (2004) 3737-3744.
[75] H. Rouault-Rogez, M. Dupeux, M. Ignat, High temperature tensile creep of CMSX-2 Nickel base superalloy single crystals, Acta Metallurgica et Materialia 42(9) (1994) 3137-3148.
[76] T. Murakumo, Y. Koizumi, K. Kobayashi, H. Harada, Creep Strength of Ni-Base Single-Crystal Superalloys on the γ/γ' Tie-Line, Superalloys, 2004.
[77] A. Baldan, Review Progress in Ostwald ripening theories and their applications to the γ′-precipitates in nickel-base superalloys Part II Nickel-base superalloys, Journal of Materials Science 37(12) (2002) 2379-2405.
[78] M.V. Nathal, Effect of initial gamma prime size on the elevated temperature creep properties of single crystal nickel base superalloys, Metallurgical Transactions A 18(11) (1987) 1961-1970.
[79] J. Yu, X. Sun, N. Zhao, T. Jin, H. Guan, Z. Hu, Effect of heat treatment on microstructure and stress rupture life of DD32 single crystal Ni-base superalloy, Materials Science and Engineering: A 460-461 (2007) 420-427.
[80] S. Sun, Q. Teng, Y. Xie, T. Liu, R. Ma, J. Bai, C. Cai, Q. Wei, Two-step heat treatment for laser powder bed fusion of a nickel-based superalloy with simultaneously enhanced tensile strength

and ductility, Additive Manufacturing 46 (2021) 102168.